

Cite this: *Food Funct.*, 2023, 14, 5805

# An aqueous olive leaf extract (OLE) ameliorates parameters of oxidative stress associated with lipid accumulation and induces lipophagy in human hepatic cells†

Tacconi S.,<sup>‡a,b</sup> Longo S.,<sup>‡c</sup> Guerra F.,<sup>c</sup> Molitani C.,<sup>b</sup> Friuli M.,<sup>d</sup> Romano A.,<sup>d</sup> Gaetani S.,<sup>d</sup> Paradiso V. M.,<sup>c</sup> Difonzo G.,<sup>e</sup> Caponio F.,<sup>e</sup> Lofrumento D.,<sup>c</sup> vergara D.,<sup>c</sup> Bucci C.,<sup>c</sup> Dini L.<sup>b,f</sup> and Giudetti A. M.  \*<sup>c</sup>

Fatty liver is a disease characterized by a buildup of lipids in the liver, often resulting from excessive consumption of high-fat-containing foods. Fatty liver can degenerate, over time, into more severe forms of liver diseases, especially when oxidative stress occurs. Olive leaf extract (OLE) is a reliable source of polyphenols with antioxidant and hypolipidemic properties that have been successfully used in medicine, cosmetics, and pharmaceutical products. Using “green” solvents with minimal impact on the environment and human health, which simultaneously preserves the extract’s beneficial properties, represents one of the major challenges of biomedical research. In the present study, we assayed the potential antioxidant and lipid-lowering effect of a “green” OLE obtained by a water ultrasound-assisted extraction procedure, on the human hepatic HuH7 cell line, treated with a high concentration of free fatty acids (FFA). We found that high FFA concentration induced lipid accumulation and oxidative stress, as measured by increased hydrogen peroxide levels. Moreover, the activity of antioxidant enzymes, catalase, superoxide dismutase, and glutathione peroxidase, was reduced upon FFA treatment. Coincubation of high FFA with OLE reduced lipid and H<sub>2</sub>O<sub>2</sub> accumulation and increased the activity of peroxide-detoxifying enzymes. OLE ameliorated mitochondrial membrane potential, and hepatic parameters by restoring the expression of enzymes involved in insulin signaling and lipid metabolism. Electron microscopy revealed an increased autophagosome formation in both FFA- and FFA + OLE-treated cells. The study of the autophagic pathway indicated OLE’s probable role in activating lipophagy.

Received 27th February 2023,  
Accepted 5th June 2023

DOI: 10.1039/d3fo00817g

rsc.li/food-function

<sup>a</sup>CarMeN Laboratory, INSERM 1060-INRAE 1397, University of Lyon, Lyon-Sud Hospital, 69310 Lyon, France. E-mail: stefano.tacconi@inrae.fr

<sup>b</sup>Department of Biology and Biotechnology “C. Darwin”, Sapienza University of Rome, P.le Aldo Moro 5, 00185 Rome, Italy. E-mail: camilla.molitani@uniroma1.it, luciana.dini@uniroma1.it

<sup>c</sup>Department of Biological and Environmental Sciences and Technologies, University of Salento, Via Prov.le Lecce-Monteroni, 73100 Lecce, Italy.

E-mail: anna.giudetti@unisalento.it, serena.longo@unisalento.it, vito.paradiso@unisalento.it, danielle.vergara@unisalento.it, dario.lofrumento@unisalento.it, flora.guerra@unisalento.it, cecilia.bucci@unisalento.it

<sup>d</sup>Department of Physiology and Pharmacology “V. Erspamer”, Sapienza University of Rome, P.le Aldo Moro 5, 00185 Rome, Italy. E-mail: marzia.friuli@uniroma1.it, adele.romano@uniroma1.it, silvana.gaetani@uniroma1.it

<sup>e</sup>Department of Soil, Plant and Food Science, University of Bari Aldo Moro, Via Amendola 165/a, 70126 Bari, Italy. E-mail: francesco.caponio@uniba.it, graziana.difonzo@uniba.it

<sup>f</sup>Research Center on Nanotechnology Applied for Engineering of Sapienza (CNIS), Sapienza University of Rome, 00185 Rome, Italy

†Electronic supplementary information (ESI) available. See DOI: <https://doi.org/10.1039/d3fo00817g>

‡These authors equally contributed to the manuscript.

## 1. Introduction

Fatty liver is a condition of excessive accumulation of lipids in the liver which can be induced, among other factors, by a high dietary intake of fats. This type of lipid accumulation, not associated with alcohol consumption, is referred to as non-alcoholic fatty liver disease (NAFLD) and can remain over-time silent. In hepatic steatosis, neutral lipids, such as triacylglycerols (TAG) and cholesterol esters, are stored in dynamic organelles called lipid droplets (LD). It has been reported that one of the prime hits responsible for the progression of NAFLD in the more severe non-alcoholic steatohepatitis (NASH) is represented by oxidative stress, a condition in which an imbalance between the production and clearance of reactive oxygen species (ROS) occurs.<sup>1</sup> Lipid accumulation can stifle mitochondrial activity with a consequent increase in the electron transport chain and ROS production. Moreover, saturated fatty acids can induce macrophage-mediated inflammation inducing Nuclear Factor kappa-light-chain-enhancer of activated B



cells (NF- $\kappa$ B)-dependent production of inflammatory cytokines such as tumor necrosis factor (TNF)- $\alpha$  and interleukin (IL)-6.<sup>2,3</sup> An excess of ROS can damage cellular structures such as proteins, lipids, and DNA leading to the onset of the disease.<sup>4</sup> Based on the clinical and experimental evidence supporting the main role of oxidative stress in the pathophysiology of NAFLD, different antioxidants have been proposed as therapeutic agents for the treatment of such diseases.<sup>5</sup>

Extra virgin olive oil represents a key component of the Mediterranean diet and many of the beneficial effects of this diet can be attributed to the high polyphenols content of the oil.<sup>6</sup> Olive leaf extract (OLE) contains a higher quantity and variety of polyphenols than commercial extra virgin olive oil.<sup>7,8</sup> In recent decades, olive leaves have been upcycled by their use in medicine, cosmetics, food, and pharmaceutical products, contributing to the olive oil chain's sustainability.<sup>9</sup> Thanks to their multifunctional properties, olive leaves represent a substrate for the more efficient extraction of antioxidants.<sup>10</sup>

Studies conducted both in animals and humans have reported beneficial effects of OLE such as antioxidant, anti-hypertensive, hypoglycemic, hypocholesterolemic, cardioprotective, anti-inflammatory, and anti-obesity.<sup>11</sup> Polyphenols are the most abundant molecules in the bioactive profile of olive leaves. The secoiridoid oleuropein is the main compound together with other secoiridoids derived from tyrosol and flavonoids.<sup>12</sup> These compounds account for the antioxidant and antimicrobial activities of OLE and could make OLE suitable for use in the food industry as a natural preservative.<sup>13</sup>

Oleuropein and its metabolite hydroxytyrosol exhibit a variety of pharmacological properties, including potent antioxidant, antiatherogenic, anti-inflammatory, antiviral, and anticancer effects. Furthermore, oleuropein and hydroxytyrosol have been shown to have an antiproliferative effect on oleic acid-induced growth of cultured intestinal cells.<sup>14</sup>

The liver is a major target organ for oxidative stress, and several experimental studies provide compelling evidence that olive oil polyphenols exhibit a beneficial hepatoprotective effect.<sup>15</sup> Indeed, a Mediterranean diet supplemented with extra-virgin olive oil has been associated with a reduced prevalence of hepatic steatosis in older individuals at high cardiovascular risk.<sup>16</sup>

The phenolic concentration in OLE strongly depends on the type of extraction process. Hence, the optimization of extraction procedures is particularly important. To maximize the recovery of phenolic compounds, parameters such as temperature and solvent composition must be considered.<sup>17</sup> The choice of solvent is the most critical step in polyphenol extraction, due to the potential consequences that it can have on the finished product. Due to polyphenol chemical composition, most solvents are represented by volatile organic compounds (such as methanol, acetone, ethyl acetate, and ethanol), which harm the environment, safety, and health.<sup>18</sup> Therefore, the research challenge in recent years has been to experiment with new greener extraction solvents that do not alter the "beneficial" potential of the polyphenolic extract. Among different extraction solvents, water appears as the greenest solvent, not only because inexpensive and environmentally benign, but

also because non-toxic, and non-flammable, providing opportunities for clean processing and pollution prevention. Moreover, water has been recommended as an extraction solvent when the extracts are used in food and pharmaceutical applications.<sup>18,19</sup>

The present work aimed to assess the potential effect of a "green" OLE, obtained with water as the extraction solvent on hepatic cells in which oxidative stress was induced by an excess of fatty acids. In this experimental condition, which mimics the hepatic steatosis consequent to a high dietary fat intake, hepatic cells accumulate fatty acids in the form of LD and undergo oxidative stress. We found that the "green" OLE had a good antioxidant effect and reduced lipid accumulation in hepatic cells. Moreover, the extract ameliorated parameters linked to mitochondrial functions. Both electron microscopy and molecular analysis indicated that most of the beneficial effects of OLE could be associated with the activation of the lipophagic pathway.

## 2. Materials and methods

### 2.1. Production and characterization of the olive leaf extract (OLE)

OLE was obtained as described in Conte, *P et al.*<sup>20</sup> Briefly, after washing, the olive leaves were dried at 120 °C for 8 minutes in a ventilated oven (Argolab, Carpi, Italy) to reach a moisture content <1%, and then ground with a blender (Waring-Commercial, Torrington, CT, USA). Milli-Q water was used as the extraction solvent in a 1/20 ratio (w/v). The extraction process was ultrasound-assisted (CEIA, Vicomaggio, Italy) and the extract was filtered through Whatman filter papers (GE Healthcare, Milan, Italy), freeze-dried (BUCHI, Switzerland, Lyovapor™ L-200), and stored at -20 °C. The total phenol content was determined using the Folin-Ciocalteu method, and the antioxidant activity was assessed by ABTS and DPPH assay protocol.<sup>21</sup> The phenolic profile was obtained by HPLC-DAD using external calibration curves with relative standards, as reported in Centrone, *M et al.*<sup>22</sup> Table 1 shows the total phenolic content (TPC), the antioxidant activity (ABTS and DPPH) of OLE expressed per g of freeze-dried extract, and the concentration of the main detected polyphenols.

### 2.2. Cell culture conditions

Hepatic HuH7 cells were cultured in low-glucose DMEM supplemented with 10% FBS, 1% stable L-glutamine, and 100 U mL<sup>-1</sup> penicillin, 100  $\mu$ g mL<sup>-1</sup> streptomycin at 37 °C in a 5% CO<sub>2</sub> atmosphere. For treatments,  $1.6 \times 10^6$  cells per well were seeded in six-well plates and grown to confluence. To emulate hepatic steatosis, 24 hours after seeding, cells were treated with a mixture of 1:2 palmitate/oleate (FFA) at the final concentration of 500  $\mu$ M (dissolved in 2 mM bovine serum albumin, BSA).<sup>23</sup> For the FFA + OLE group, cells were incubated with the FFA mixture together with OLE. All experiments were made with 0.1 mg mL<sup>-1</sup> OLE. Cells treated only with the vehicle (BSA) were used as a control (CTR) and another group of cells (OLE) were incubated only with the leaf extract to evalu-



**Table 1** Total polyphenolic content (TPC), antioxidant activity (ABTS, DPPH), and polyphenol concentrations

Parameters	Concentrations
TPC (mg GAE g <sup>-1</sup> )	128 ± 1
ABTS (μmol TE g <sup>-1</sup> )	709 ± 9
DPPH (μmol TE g <sup>-1</sup> )	680 ± 3
Compounds	Concentrations (mg g <sup>-1</sup> )
Oleuropein	95 ± 2
Verbascoside	17 ± 3
Apigenin-7-O-glucoside	5 ± 1
Rutin	4 ± 1
Tyrosol	3 ± 0
Luteolin-7-O-glucoside	2 ± 0

GAE = gallic acid equivalents; TE = trolox equivalents.

ate its effects in the absence of a pro-oxidant stimulus. All treatments were performed for 48 hours. Nuclei and cytosol fractions were isolated as reported in Giudetti, AM *et al.*<sup>24</sup>

### 2.3. UHPLC–ESI-MS/MS analysis of oleuropein in culture medium

The culture medium was filtered through 0.45 μm polytetrafluoroethylene filters. The oleuropein content in the medium during incubation (0, 4, 24, 48 hours) was monitored by ultra-high performance liquid chromatography–electrospray tandem mass spectrometry (UHPLC–ESI-MS/MS, Thermo Fischer Scientific, Waltham, MA, USA). MS conditions were capillary temperature 320 °C; source heater temperature 280 °C; nebulizer gas N<sub>2</sub>; sheath gas flow 30 psi; auxiliary gas flow 7 arbitrary units; capillary voltage –2800 V, S-Lens RF Level 60%. Data were acquired in negative ionization mode. A full scan method from 100 to 900 *m/z* was used to quantify the phenolic compounds by the extraction of molecular ion signals in post-acquisition. All data were acquired and processed using Xcalibur v.2 (Thermo Fischer Scientific). The identification was performed also by comparing the data with those reported by Difonzo, G *et al.*<sup>25</sup> The quantitation was performed as described in Centrone, M *et al.*<sup>22</sup>

### 2.4. Cell proliferation and viability assay

After incubation with OLE, cell viability was measured using a ReadyProbes™ Cell Viability Imaging Kit (ThermoFisher #R37609). After treatments, HuH7 cells were incubated with 2 drops of each cell stain reagent for 15 min. NucBlue® Live reagent stained the nuclei of all the cells and was detected with a standard DAPI filter. NucGreen® Dead reagent stained only the nuclei of cells with compromised plasma membrane integrity and was detected using a standard FITC/GFP (green) filter. The number of cell nuclei with compromised plasma membrane integrity was determined and averaged in three areas, measuring 0.01 mm<sup>2</sup>, by fluorescent microscopy. Sulforhodamine B (SRB) colorimetric assay was used to analyze cell proliferation. In this case, after incubation with OLE, cells were fixed with 50% trichloroacetic acid for 1 h at 4 °C and washed with water.

After completely drying at room temperature, the cells were stained for 30 min with 0.4% (w/v) SRB dissolved in 1% acetic acid. The plate was washed four times with 1% acetic acid to remove the unbound dye. The viable cell number was directly proportional to the protein bound-dye formation which was then solubilized with 10 mM Tris base solution pH 10.5 and measured at 570 nm on a microplate reader (BioTek Cytation 5 Cell Imaging Multimode Reader, Agilent). Cell growth inhibition at three different times was evaluated as the ratio between the average value of the absorbance at 570 nm obtained in treated and untreated cells × 100.

### 2.5. Western blot analysis

Total proteins were extracted from HuH7 cells using a protein extraction buffer. Following centrifugation at 12 000g for 10 minutes at 4 °C, supernatants were collected and assayed for protein content using the Bradford method. In total, 30 μg protein was loaded onto a lane of a sodium dodecyl sulfate (SDS) gel and subsequently subjected to electrophoretic separation. Proteins were transferred to nitrocellulose membranes (Amersham) at 4 °C and 100 V for 80 minutes. Next, membranes were blocked using 5% (w/v) powdered milk for 1 hour and incubated with primary antibodies. Rabbit polyclonal anti-nuclear factor kappa-light-chain-enhancer of activated B cells (p65) (NF-κB (p65), Santa Cruz sc-84141, mouse 1:1000), Insulin Receptor (IR, GeneText GXGTX101136, rabbit 1:1000), Glycogen Synthase (GS, Santa Cruz sc-81173, mouse 1:1000), Diacylglycerol Acyltransferase 2 (DGAT2, Novus Biologicals, #NBP1-71701, mouse 1:1000), Monoacylglycerol Lipase (MAGL, Santa Cruz sc-398942, mouse 1:1000), Adipose Triglyceride Lipase (ATGL, Santa Cruz, mouse 1:1000), Stearoyl-CoA Desaturase 1 (SCD1, Santa Cruz #sc-58420, Mouse 1:1000), Microtubule-Associated Protein 1α/1β-Light Chain 3 (MAP LC3α/β (G-4) Santa Cruz #sc-398822, Mouse 1:1000) and p62 (SQSTM1/p62 (D-3) Santa Cruz #sc-28359, Mouse 1:1000) were used. Beta-actin (Bioss Antibodies #bs-0061R, Rabbit 1:1000), alpha-tubulin (Santa Cruz sc-5286, Human 1:10.000), and lamin A/C (Santa Cruz, sc-71481 1:5000) were used as housekeeping proteins. After washing with Tris-Buffer Saline added with 0.1% Tween 20 (TTBS), the blots were incubated with peroxidase-conjugated secondary antibodies (Sigma-Aldrich) at 1:10.000 dilutions at room temperature for 1–2 h. The blots were then washed thoroughly in TTBS. Western blotting analyses were performed using Amersham ECL Advance Western Blotting Detection Kit (GE Healthcare, Little ChaeAnt, UK). Densitometric analysis of the immunoblots was performed using Image Lab™ Version 6.0.1 2017 (Bio-Rad Laboratories, Inc.) software.

### 2.6. Lipid droplet staining and measurements

All experimental groups were processed for Oil Red-O staining for LD visualization and immunostaining to analyze LC3 distribution. After treatments, cells were washed three times with PBS and incubated with 4% paraformaldehyde in PBS pH 7.4 for 5 minutes, at room temperature. After three more washes, samples were stained with 5% Oil-O-Red solution in isopropyl



alcohol for 1 hour at room temperature and washed again with PBS.

Quantification and area measurements of LD were performed with ImageJ software (Version 1.50i, Bethesda, MD, USA). For separation of the LD foreground from the background and diffuse cellular staining, the 12-bit images were converted to 8-bit, Gaussian blurred with sigma set to 1, and a threshold of 25 was applied. After thresholding, the image was converted to a binary mask, adjacent objects were separated using the watershed function, and the analyze particle function was used to record each droplet as a region of interest (ROI) corresponding to a single cell.

For LC3 immunostaining, Oil-O-Red-stained samples were permeabilized with Triton X-100 for 30 minutes to allow the antibody to penetrate, then samples were incubated with 5% BSA for one hour to reduce the nonspecific antibody binding. After blocking, cells were incubated with specific primary anti-LC3 overnight at 4 °C. The cells were washed thrice with PBS for 5 minutes each time, followed by incubation with a goat anti-mouse IgG FITC-conjugated (1 : 250, ab6785; Abcam) secondary antibody for 60 minutes at room temperature in the dark. DAPI was used to stain the nucleus of hepatocytes. The images were captured with a fluorescence microscope Axio Observer (Zeiss) equipped with Apotome 3 (40× objective), and fluorescence intensity was analyzed with FIJI (Version 2.9.0/1.53t).

BODIPY staining was performed as described.<sup>26,27</sup> Briefly, cells were washed with PBS and incubated with 5 μM BODIPY 493/503 for 15 min at 37 °C. After that, cells were washed twice with PBS and then fixed, permeabilized, and stained with the appropriate antibodies as previously described.<sup>28</sup> The used primary antibody was anti-LAMP1 (1 : 250, H4A3, deposited to the Developmental Studies Hybridoma Bank (University of Iowa, Iowa City, IA, USA by J.T. August and J.E.K. Hildreth). Images were captured with Zeiss LSM700 confocal laser scanning microscope (Zeiss, Oberkochen, Germany) equipped with a 63×/1.40 NA oil immersion objective. Lysosome number was determined by ImageJ software (Version 1.50i, Bethesda, MD, USA) and was calculated as a count of dots per cell.<sup>29,30</sup> Measures were obtained by analyzing at least 20 cells per sample in at least three independent experiments.

### 2.7. Reactive oxygen specie (ROS) and TNF-α measurements

To detect the changes in intracellular ROS levels, 2',7'-dichlorofluorescein diacetate (DCFH-DA, Sigma-Aldrich) staining was used.<sup>31</sup> DCFH-DA is a stable, fluorogenic, and non-polar compound that can readily diffuse into the cells and get deacetylated by intracellular esterases to a non-fluorescent 2',7'-dichlorodihydrofluorescein (DCFH) which is later oxidized by intracellular ROS into highly fluorescent 2',7'-dichlorofluorescein (DCF). The intensity of fluorescence is proportional to intracellular ROS levels. HuH7 cells were seeded at a density of  $2 \times 10^5$  cells per well in 24 well plates and were allowed to attach overnight. On the first day of treatment, the medium was replaced with fresh ones containing BSA (CTR), FFA, and FFA + OLE. After 48 h the medium was removed, cells were

washed once with fresh DMEM, and twice with 1× PBS and incubated with 10 μM DCFH-DA for 30 minutes. Cells were rinsed with PBS and representative fluorescent images for each well using the green fluorescent protein (GFP) channel on an Evos m7000 fluorescence microscope were taken. After taking images, PBS was removed and a radioimmunoprecipitation assay (RIPA) buffer was added to each well. The collected cells were incubated at -80 °C for 20 minutes and then centrifuged at 21 130g for 10 minutes at 4 °C. The collected supernatant was transferred to a black 96-well plate. The fluorescence intensity was measured using the CLARIOstar Plus microplate reader at an excitation wavelength of 485 nm and an emission wavelength of 530 nm. After fluorescence recording, 5 μL of supernatant was transferred to a 96-well well plate containing 195 μL of 1× protein assay solution to measure the protein concentration with the Bradford method. The fluorescence intensity was normalized to the protein concentration.

TNF-α level was evaluated in cell culture supernatants from HuH7 cells. Enzyme-linked immunosorbent assay (ELISA) kits were used according to the manufacturer's instructions (R&D Systems, Minneapolis, MN).

### 2.8. Mitochondrial membrane potential measurements

To determine mitochondrial membrane potential the meta-chromatic fluorophore JC-1, a lipophilic cation able to cross cell membranes was used. When mitochondria display an intact potential, JC-1 is attracted by the mitochondrial matrix negative charges, forming the so-called J-aggregates, with red fluorescence (ex.: 490 nm; em.: 590 nm). When the mitochondrial membrane depolarizes, JC-1 accumulates in its monomeric forms in the cytosol, displaying a green fluorescence (ex.: 490 nm; em.: 527 nm). To stain cells 1 mg mL<sup>-1</sup> of JC-1 stock solution diluted in DMSO was used, and after 30 minutes of incubation, samples were washed and at least fixed with 1% formaldehyde for 5 minutes. Observations were performed with a fluorescence microscope Axio Observer (Zeiss) equipped with Apotome 3, and the red/green fluorescence ratio (used as mitochondrial functionality index) was quantified with FIJI (Version 2.9.0/1.53t).

### 2.9. Enzyme activity assays

HuH7 cells were collected 48 hours after treatments. The activities of hepatic transaminases alanine transaminase (ALT) and aspartate transaminase (AST) were determined by using commercial kits (Merck KGaA, Darmstadt, Germany). Glutathione peroxidase (GPx), catalase (CAT), and superoxide dismutase (SOD) activities were assayed as reported in Giudetti, AM *et al.*<sup>24</sup> Specifically, GPx activity was assayed by following the instructions reported in Cayman's GPx assay kit (Cayman Chemical, Ann Arbor, MI, USA). The activity was measured indirectly by a coupled reaction with glutathione reductase. Oxidized glutathione (GSSG) produced upon reduction of hydroperoxide by GPx is recycled to its reduced state by glutathione reductase (GR) and nicotinamide adenine dinucleotide phosphate (NADPH). The change in absorbance at 340 nm was monitored for 3 minutes. A blank with all ingre-



dients except the sample was also monitored. Specific activity was calculated as U mg<sup>-1</sup> protein. CAT activity was measured with a catalase assay kit (cat. no. #219265, Sigma-Aldrich) that uses a reaction between the catalase present in the sample and H<sub>2</sub>O<sub>2</sub> to produce water and oxygen. The unconverted H<sub>2</sub>O<sub>2</sub> reacts with a probe to generate a product that can be measured spectrophotometrically at 540 nm. SOD activity was assayed by a Kit (cat. no. 19160, Sigma-Aldrich), which utilized a tetrazolium salt for the detection of superoxide radicals generated by xanthine oxidase and hypoxanthine. SOD activity was calculated using the equation obtained from the linear regression of a standard curve built in the same experimental conditions.

### 2.10. Transmission electron microscopy (TEM) analysis

After treatments, cells were fixed with 2.5% glutaraldehyde in 0.1 M cacodylate buffer pH 7.4 for one hour and post-fixed with 1% OsO<sub>4</sub> in the same buffer for two hours in ice. After fixation, cells were dehydrated with ethanol (25%, 50%, 70%, 90%, and 100%) and embedded in Spurr resin. Ultra-thin sections (60 nm) will be deposited on a 200-mesh copper grid and observed under an electron microscope Hitachi 7700 (Hitachi High Technologies America Inc., Dallas, TX) transmission electron microscope operating at 100 kV.

### 2.11. Statistical analysis

Statistical analyses were conducted by one-way ANOVA followed by Tukey's *post hoc* analysis (Graph-pad Prism 8). Values were expressed as means ± SD; *p*-values <0.05 were significant.

## 3. Results

### 3.1. OLE reduces lipid accumulation and ameliorates liver parameters in FFA-treated cells

Preliminarily, we evaluated the cytotoxic potential of OLE at five different concentrations (0.01–0.05–0.1–0.5 and 1.0 mg mL<sup>-1</sup>) and three times (12–24 and 48 hours). Only the highest concentration (1.0 mg mL<sup>-1</sup>), regardless of incubation times, significantly reduced cell viability (Fig. 1S†). Therefore, all experiments were conducted at 48 hours with 0.1 mg mL<sup>-1</sup> OLE, a concentration that has been shown to have high potential antioxidant efficacy in bronchial epithelial NCI-H292 cells.<sup>21</sup>

Oleuropein, which is the major component of OLE (Table 1), is an ester of hydroxytyrosol and elenolic acid glucoside.<sup>32,33</sup> We analyzed whether oleuropein, added to HuH7 cells, could undergo a hydrolysis process during the experimental period. For this purpose, HuH7 cells were incubated with 0.1 mg mL<sup>-1</sup> of OLE and the medium was analysed at different time points. During the incubation time, the amount of oleuropein steadily decreased and, already at 4 hours, a reduction of approximately 30% was measured. Subsequently, the decrease in oleuropein was associated with the appearance in the medium of a compound identified, by UHPLC–ESI-MS, as elenolic acid glucoside ([M – H]<sup>-</sup> = 403.1) (Table 1S†).

OLE incubated for 48 hours with HuH7 cells significantly reduced FFA-induced lipid accumulation, as evidenced by the decrease in fluorescence intensity associated with LD staining (Fig. 1A and B), LD number, and LD area, compared with CTR cells (Fig. 1C and D). Additionally, OLE improved parameters associated with liver functionality, as demonstrated by a recovery of ALT and AST transaminase activities, which were significantly higher than CTR in FFA-treated cells (Fig. 1E). OLE, alone, did not affect measured parameters, thus indicating a specific effect of the extract on abnormalities induced by the high FFA load.

### 3.2. OLE influences insulin signaling and lipid metabolism in FFA-treated cells

Lipid metabolism is regulated by insulin and accumulated TAG can induce insulin resistance,<sup>34</sup> a feature of NAFLD.<sup>35</sup> We followed the expression of insulin receptor (IR) and the downstream glycogen synthase (GS) protein, in differently treated cells.

The excess of FFA strongly reduced both IR and GS expression (Fig. 2A–C), thus indicating reduced insulin responsiveness of FFA-treated cells. Co-incubation of FFA with OLE reported both IR and GS to control values. OLE alone did not modify both IR and GS protein expression in confront to CTR thus indicating a specific effect of the extract on FFA-induced hepatic disruption of insulin signaling.

Considering the altered insulin pathway and increased lipid accumulation, we followed the expression of specific regulatory enzymes of lipid metabolism. The protein expression of SCD1, involved in the conversion of saturated to monounsaturated fatty acids (main substrates of the TAG synthesis), was significantly increased, with respect to CTR, by the excess of FFA and brought back to CTR by OLE (Fig. 2D).

Furthermore, we measured the expression of DGAT2, a key enzyme in TAG synthesis, ATGL involved in the hydrolysis of TAG to diacylglycerols and FFA and MAGL which catalyze the conversion of monoacylglycerols to glycerol and FFA. With respect to CTR, high FFA concentration significantly increased DGAT2 and MAGL and decreased ATGL expressions. In all cases, the addition of OLE abolished the alterations induced by FFA (Fig. 2A and E–G). OLE alone significantly increased ATGL expressions with respect to CTR thus indicating a protective effect of the extract even in control hepatocytes.

### 3.3. OLE influences mitochondrial functionality and oxidative stress in FFA-treated cells

Oxidative stress and ROS accumulation can lead to alterations in the mitochondrial structure/function. Labeling with the JC-1 probe is useful in analyzing mitochondrial membrane potential, a crucial parameter for evaluating mitochondrial functionality. With respect to CTR, the high FFA concentration significantly decreased the mitochondrial membrane potential in HuH7 cells, as measured by a decreased JC-1 red/green ratio (Fig. 3A and B). In addition, compared to CTR, FFA increased intracellular ROS levels (Fig. 3C) and decreased the activities of antioxidant enzymes CAT, SOD, and GPx (Fig. 3D–F). Co-incu-



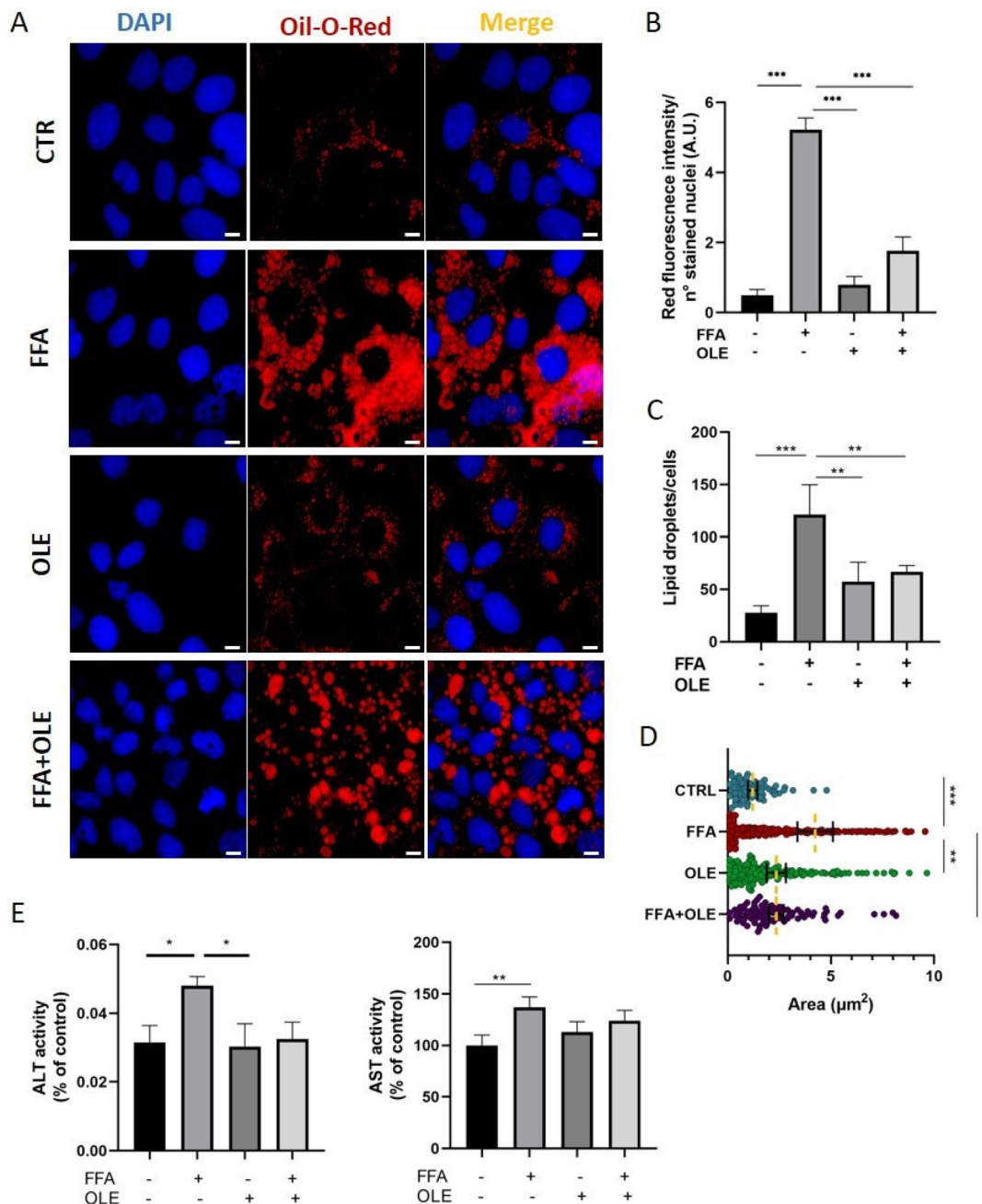


**Fig. 1** OLE effects on lipid accumulation, and liver parameters. (A) Representative microscopic images of Oil-O-red-stained HuH7 cells (scale bar 5  $\mu\text{m}$ ) untreated (CTR) and treated with high fatty acids (FFA), 0.1  $\text{mg mL}^{-1}$  leaf extract (OLE), and FFA + OLE and (B) relative quantification. (C and D) Lipid droplet amount and area have been determined as reported in Materials and Methods. The yellow dotted lines in the LD area panel represent the median values for each experimental group. A total of five images were analyzed for each experimental group, in three different experiments. (E) Alanine transaminase (ALT) and aspartate transaminase (AST) activities have been measured in untreated cells and treated with FFA, 0.1  $\text{mg mL}^{-1}$  OLE 0.1 and FFA + OLE. Values are expressed as % of controls. Each value represents the mean  $\pm$  SD of three independent experiments. \* $p < 0.05$ , \*\* $p < 0.005$ , \*\*\* $p < 0.001$ .

bation of FFA-treated cells with OLE resulted in a significant recovery of the membrane potential with a concomitant decrease in  $\text{H}_2\text{O}_2$  level. Moreover, all enzymatic activities related to the peroxide detoxification were recovered by OLE treatment. Note that the effect of the extract was specifically associated with the reduction of oxidative stress induced by

lipid accumulation because OLE, alone, did not change either the  $\text{H}_2\text{O}_2$  level or the antioxidant enzyme activities, compared with CTR.

It is known that intracellular ROS can regulate the NF- $\kappa\text{B}$  response, and NF- $\kappa\text{B}$  target genes can affect the production of ROS.<sup>36</sup> To further explore the mechanism of the antioxidant



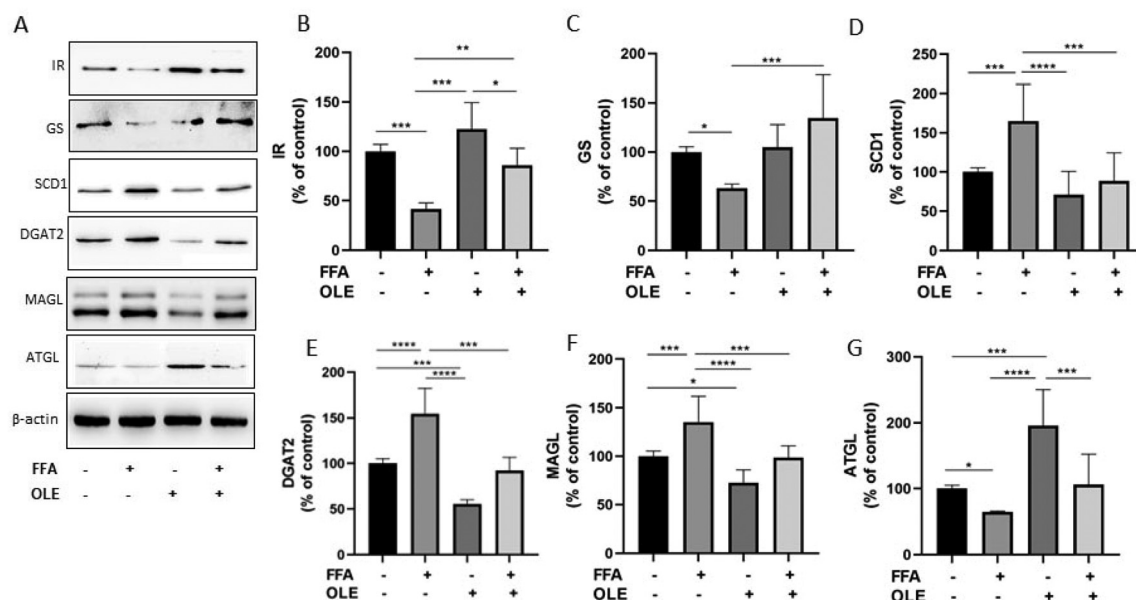


**Fig. 2** OLE on insulin signaling and lipid metabolism. (A) Representative image of western blot analysis of insulin receptor (IR), glycogen synthase (GS) stearoyl-CoA desaturase 1 (SCD1), diacylglycerol acyltransferase 2 (DGAT2), monoacylglycerol lipase (MAGL) and adipose triacylglycerol lipase (ATGL) obtained from HuH7 cells untreated and treated with high fatty acids (FFA), 0.1 mg mL<sup>-1</sup> olive leaf extract (OLE) and FFA + OLE. (B–G) Quantitative analysis of IR, GS, SCD1, DGAT2, MAGL, ATGL. Values are reported as % of controls and represent the mean ± SD of five independent experiments. \**p* < 0.05, \*\**p* < 0.005, \*\*\**p* < 0.001; \*\*\*\**p* < 0.0001.

potential of OLE, we assessed the extent of the NF-κB p65 nuclear translocation after the addition of OLE to FFA-treated cells. We observed that FFA enriched the nuclear abundance of NF-κB p65 as compared with CTR, and OLE addition significantly increased, with respect to FFA-treated cells, the nuclear translocation of NF-κB p65 (Fig. 3G and H).

Activation of the NF-κB pathway is often associated with high circulating levels of pro-inflammatory cytokines such as TNF, IL-6, and IL-1β.<sup>37,38</sup> To determine to what extent OLE can modify the FFA-induced inflammatory response, we measured the amount of TNF-α released in the cultured medium of HuH7 cells exposed to high FFA and OLE. We found that OLE significantly decreased the FFA-induced inflammatory response as indicated by the lower TNF-α level released in the medium of FFA + OLE with respect to FFA-treated cells (Fig. 3I).

### 3.4. OLE induces lipophagy in FFA-treated cells

Through TEM analysis, substantial morpho-structural differences between FFA, FFA + OLE, and CTR cells, were observed. TEM micrographs (Fig. 4) show an increase in the amount and size of LD within FFA-treated cells compared to CTR, with a round shape morphology and an evident electron-dense protein coating. This accumulation of LD was much less evident in the FFA + OLE group and completely absent in cells treated only with OLE (Fig. 4). Additionally, compared to CTR, autophagosomes (AP) with variable sizes and autophagosomes containing LD (LAP, lipophagosome) were observed in the FFA group. However, more AP and LAP were observed in the

FFA + OLE group compared to CTR and FFA-treated cells (Fig. 4).

Previous studies have demonstrated that NAFLD can induce mitochondrial dysfunction and autophagy arrest.<sup>39–41</sup> Based on the above-reported data, we decided to investigate the role of FFA and OLE on the autophagy process by measuring the protein expression of LC3 and p62. Moreover, we also simultaneously analyzed the expression of LC3 linked to the accumulation of LD by immunofluorescence coupled with Oil-O-Red staining. Fluorescent images obtained with LC3 antibody and red oil staining of differently treated HuH7 cells demonstrated an increase in fluorescence associated with LD in FFA-treated cells (red fluorescence), confirming our above-reported data. The LD-associated fluorescence intensity significantly decreased after OLE addition (Fig. 5B). Moreover, increased fluorescence associated with LC3 antibody, localized to Oil-O-Red positive areas, in both FFA- and FFA + OLE-treated cells, was also measured (Fig. 5A and B). In addition, treatments of HuH7 cells with FFA and FFA + OLE increased the expression and LC3-II/LC3-I ratio in confront to CTR (Fig. 5C and E). A significant increase also in the p62 protein expression was measured in FFA-treated cells, compared to untreated cells. The addition of OLE to FFA-treated cells significantly reduced LC3-II/LC3-I ratio compared to FFA. Finally, to confirm these data, we analyzed the recruitment of LD in LAMP1-positive lysosomes through BODIPY staining followed by immunostaining of the degradative compartment.<sup>26,27</sup> Indeed, the primed autophagic LD fuse with late endosomes and lysosomes to eventually form an autolysosome for lipid degradation.<sup>42,43</sup> After FFA treatment, a significant reduction



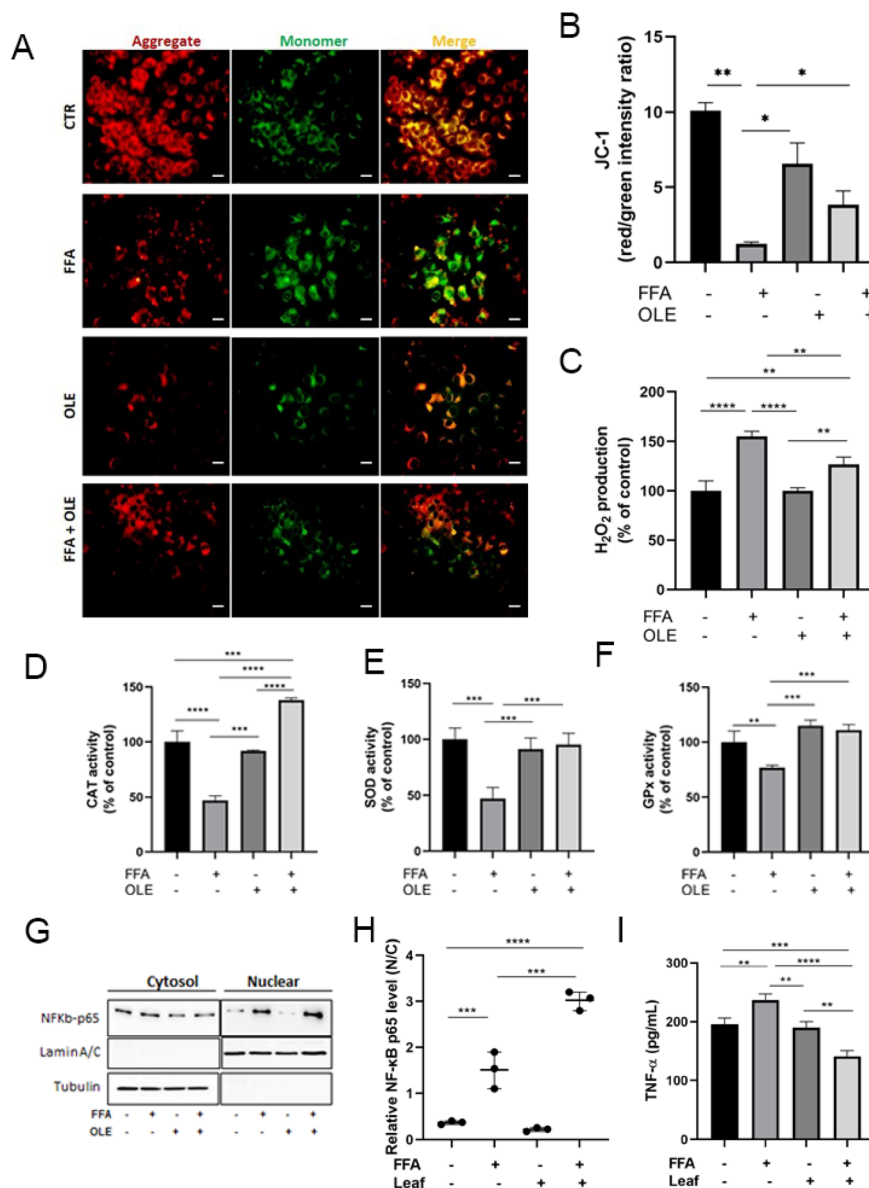


**Fig. 3** OLE on mitochondrial membrane potential, oxidative stress, and inflammatory parameters. (A) Representative images of JC-1 labeled HuH7 cells untreated and treated with high fatty acids (FFA), 0.1 mg mL<sup>-1</sup> olive leaf extract (OLE), and FFA + OLE obtained by fluorescent microscopy (scale bar 50  $\mu$ m). (B) Quantification of the mitochondrial membrane potential, by FIJI (Version 2.9.0/1.53t). (C) Hydrogen peroxide measurement with DCFH-DA in untreated cells and treated with FFA, 0.1 mg mL<sup>-1</sup> OLE, and FFA + OLE. (D–F) Enzymatic activity assay of catalase (CAT) superoxide dismutase (SOD) and glutathione peroxidase (GPx) in HuH7 cells no treated and treated FFA, OLE 0.1 mg mL<sup>-1</sup>, and FFA + OLE. (G–H) Nuclear and cytosol distribution of NF- $\kappa$ B-p65 and relative quantification in HuH7 cells untreated and treated with FFA, 0.1 mg mL<sup>-1</sup> OLE and FFA + OLE. (I) Tumor Necrosis Factor- $\alpha$  (TNF- $\alpha$ ) levels in culture medium. Values represent the mean  $\pm$  SD of three different experiments, \* $p$  < 0.05, \*\* $p$  < 0.005, \*\*\* $p$  < 0.001.

(about 50%), with respect to the CTR, in LAMP1-positive compartments, was found (Fig. 5G panels c, and d and Fig. 5F). Interestingly, a recovery of the lysosomal abundance was found after the treatment of FFA cells with OLE (Fig. 5G, panels g and h, and Fig. 5F). BODIPY staining showed similar behavior in both CTR and OLE-treated cells, in which LD appear surrounded by LAMP-1 positive compartments (Fig. 5G, panels b, and f). No colocalization between LD and degradative compartments was found in FFA-treated cells. In addition, a reduced number of lysosomes was measured in FFA-treated

cells with respect to CTR (Fig. 5G, panel d, and Fig. 5F). OLE treatment of FFA cells induced recovery in lysosomes and the emergence of LD surrounded by LAMP1-marked compartments, indicating activation of lipophagy (Fig. 5G, panel h).

## 4. Discussion

In this study, the antioxidant potential of a “green” OLE on oxidative stress induced by an excess of FFA, in hepatic human





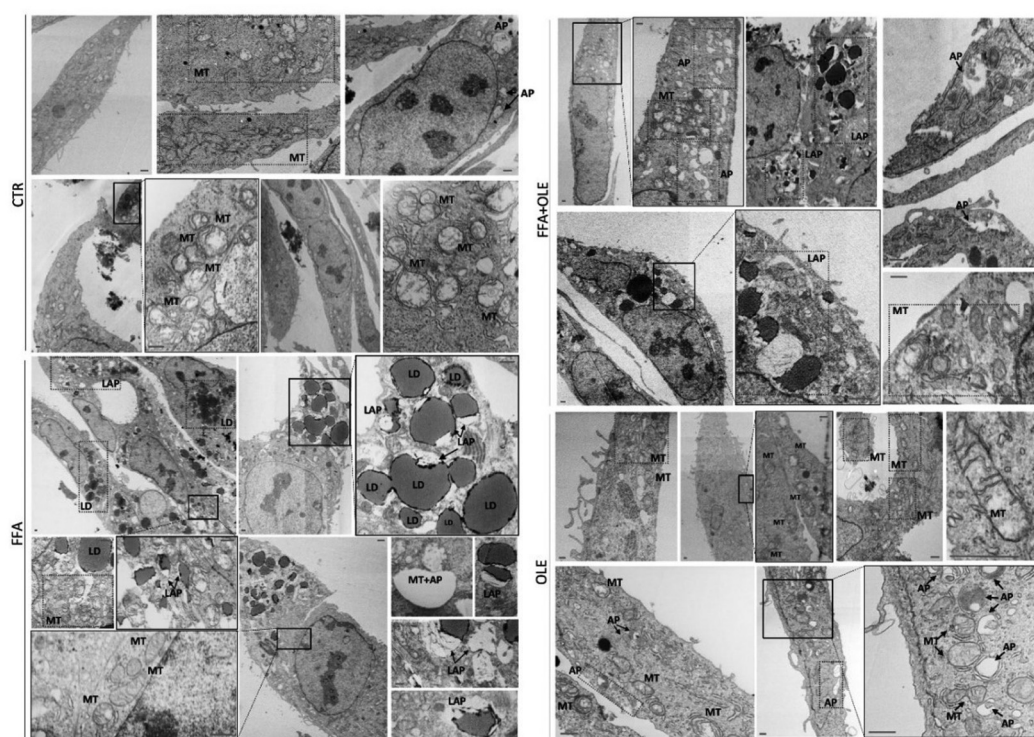


**Fig. 4** Transmission electron microscopy (TEM) images. HuH7 cells untreated (CTR) and treated with high fatty acids (FFA), 0.1 mg mL<sup>-1</sup> olive leaf extract (OLE) and FFA + OLE. MT, mitochondrion; LD, lipid droplet; AP, autophagosome; LAP, lipoautophagosome (scale bar 500  $\mu$ m).

HuH7 cells, has been evaluated. As indicated in Table 1, the main compound in OLE is oleuropein. *In vitro* and *in vivo* studies have reported several health-promoting effects of oleuropein.<sup>44</sup> Recent epidemiological and experimental studies described the beneficial effects of oleuropein derived from olive trees on different diseases.<sup>45</sup> However, it must be considered that oleuropein is the main precursor of hydroxytyrosol, to which numerous positive effects have also been attributed.<sup>46</sup> The antioxidant properties of the products and by-products of olive leaf extracts have been clearly demonstrated, and the most potent scavenger actions against superoxide anion and other reactive species have been demonstrated for oleuropein and hydroxytyrosol.<sup>47</sup> To this respect, a recent work reports a protective effect of hydroxytyrosol against reactive oxygen species together with an antiproliferative effect in adenocarcinoma cell cultures.<sup>48</sup> We found that the amount of added oleuropein rapidly decreased during the incubation, and elenolic acid glucoside, one of its hydrolysis products, began to appear later in the medium. Although hydroxytyrosol is, together with elenolic acid, a hydrolysis product of oleuropein, we did not detect it, probably due to its rapid metabolization by liver cells.<sup>49</sup> Therefore, we cannot exclude that most of the biological effects we observed in our experimental conditions are due to both oleuropein and its hydrolysis products, as well as to minor olive oil constituents, as reported.<sup>50</sup>

It is well known that elevated lipid levels lead to lipotoxicity and oxidative stress in the liver.<sup>51</sup> This condition is often

associated with the impairment of antioxidant status both *in vitro* and *in vivo*.<sup>52</sup> In the present study, excess FFA increased ROS levels in the liver and reduced total antioxidant capacity, as indicated by a decrease in antioxidant enzyme activity. Studies have demonstrated the antioxidant effects of olive leaf extract against NAFLD,<sup>53</sup> NASH occurrence,<sup>54</sup> and high-fat diet-induced metabolic disorders.<sup>55</sup> Moreover, polyphenols from extra-virgin olive oil have been reported to reduce oxidative stress induced by elevated fatty acids.<sup>56</sup> We found that OLE ameliorated oxidative stress induced by high FFA treatments in liver cells by lowering H<sub>2</sub>O<sub>2</sub> levels and restoring antioxidant enzyme activities.

Sustained levels of ROS can induce alterations in mitochondrial functions and morphology and the opening of mitochondrial transition pores with a loss of the mitochondrial membrane potential.<sup>57,58</sup> We can argue that the decrease in ROS production in OLE-treated cells can prevent mitochondrial damage and the membrane potential drop we measured after excess FFA addition. Our data agree with those obtained by *in vivo* and *in vitro* experiments reporting a protective role of olive oil and its phenolic components on mitochondrial membrane potential and functions.<sup>59–62</sup> Moreover, the decrease in lipid accumulation after OLE treatments can be responsible for the ameliorative effect on insulin signaling we measured. This latter result is in keeping with previous observations suggesting that oleuropein decreases insulin resistance and prevents the progression of NASH to fibrosis.<sup>44</sup>



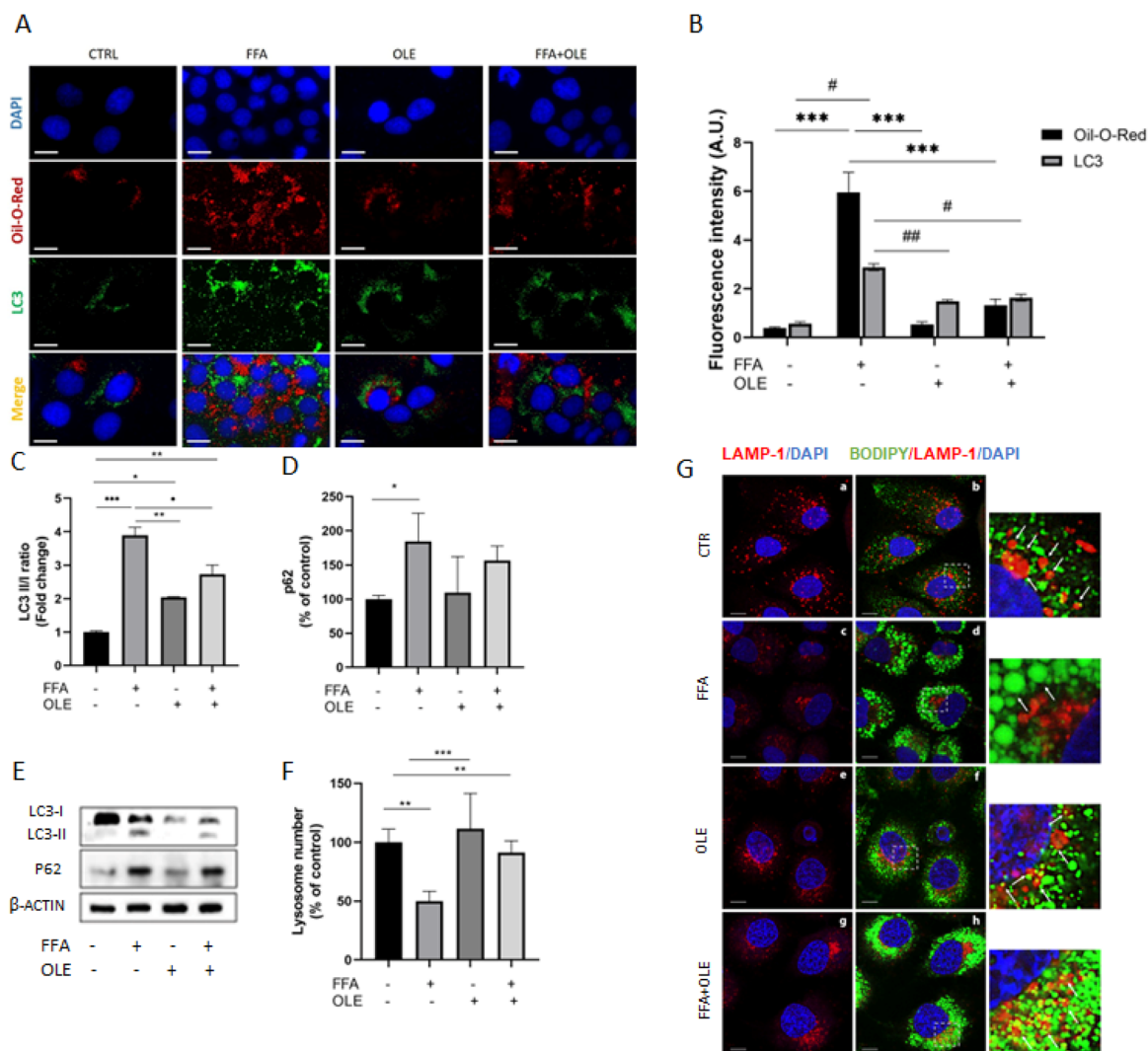


**Fig. 5** OLE influences autophagy parameters. (A) Fluorescence microscopy of HuH7 cells untreated (CTR) and treated with high fatty acids (FFA),  $0.1 \text{ mg mL}^{-1}$  olive leaf extract (OLE), and FFA + OLE stained with both LC3 and Oil-O-red and (scale bars  $10 \mu\text{m}$ ) and (B) relative quantification. Asterisk (\*) refers to Oil-O-Red and hashtag (#) to LC3 statistics. (C–E) Western blot analysis and relative quantification of LC3-I and LC3-II isoforms and the p62 protein from HuH7 cells untreated and treated with high fatty acids (FFA),  $0.1 \text{ mg mL}^{-1}$  olive leaf extract (OLE), and FFA + OLE. Values represent the mean  $\pm$  SD of three independent experiments. (F) Lysosome quantification from immunofluorescence analysis. Values have been obtained by analyzing at least 50 cells per sample in four different experiments. (G) Representative images of LD interaction with lysosomes investigated by immunofluorescence analysis using BODIPY 493/503 to label LD (green) and anti-LAMP-1 (red) antibodies in control cells (CTR) and in cells treated with FFA, OLE  $0.1 \text{ mg mL}^{-1}$ , and FFA + OLE. Nuclei were stained with DAPI (blue). White boxes indicated zoomed areas on the right. White arrows point to LD. Values are the mean  $\pm$  SD of four different experiments. Scale bar =  $10 \mu\text{m}$ . \* $p < 0.05$ , \*\* $p < 0.005$ , \*\*\* $p < 0.001$ .

To alleviate oxidative damage, cells activate defense mechanisms and the NF- $\kappa$ B system is crucial in this respect.<sup>63</sup> Indeed, a correlation between NF- $\kappa$ B and ROS has been reported.<sup>63</sup> Different studies have shown that an excessive accumulation of ROS can activate the NF- $\kappa$ B pathway and this, in turn, can influence the expression of antioxidant proteins.<sup>63</sup> After stimulation, NF- $\kappa$ B detaches from the inhibitory I $\kappa$ B subunit and translocates to the nucleus, where regulates the transcription of target genes.<sup>64</sup> The p65 subunit of NF- $\kappa$ B is the strongest activator of most NF- $\kappa$ B-responsive genes.<sup>65</sup> Our results showed that OLE increased the nuclear level of p65 in hepatic cells above the value measured in FFA-treated cells.

Considering that the NF- $\kappa$ B pathway has been reported to influence ROS levels by upregulating antioxidant proteins, such as Mn-SOD and GPx,<sup>63</sup> we can postulate that the increased nuclear translocation of p65, observed after OLE treatments, might account for the increased activity of antioxidant enzymes measured in our experiments. Our data confirmed the involvement of the NF- $\kappa$ B pathway in the antioxidant effect of olive leaf extract and olive oil polyphenols has already been reported.<sup>66,67</sup> We found that the addition of OLE to FFA-treated cells prevents the alteration induced by FFA on the expression of key proteins involved in TAG metabolisms such as SCD1, DGAT2, MAGL, and ATGL. SCD1 furnishes the



main substrates for TAG synthesis by desaturating saturated fatty acids into monounsaturated ones. Several studies have demonstrated that SCD1 plays a key role in the development of NAFLD,<sup>68</sup> and deletion of SCD1 protects against diet-induced adiposity and hepatic steatosis.<sup>69</sup> DGAT2 participates in the latest step of TAG synthesis. Its expression has been reported to be upregulated in hepatic steatosis.<sup>70</sup> DGAT2 but not DGAT1 isoform is primarily involved in the accumulation of TAG during NAFLD.<sup>70</sup> MAGL is the rate-limiting enzyme of monoacylglycerol degradation, generating glycerol and fatty acids. Inhibition of MAGL has been shown to have a protective effect on different liver diseases. In diet-induced obesity models, MAGL ablation showed to be protective in the development of glucose intolerance and insulin resistance.<sup>71</sup> Finally, ATGL expression has been reported to be decreased in the liver of steatosis patients,<sup>72</sup> and ATGL up-regulation enhances liver insulin sensitivity.<sup>73</sup> We found that high FFA concentration induced up-regulation of SCD1, DGAT2, and MAGL and down-regulated ATGL, coherent with the role of FFA in inducing hepatic steatosis. In all cases, OLE prevented the effect induced by FFA. Note that MAGL, catalyzing the hydrolysis of 2-arachidonoylglycerol to arachidonic acid, the precursor for prostaglandin synthesis, is also involved in the modulation of the inflammatory pathway.<sup>74</sup> Altogether these results confirm a primary role of OLE in TAG metabolism and inflammation supporting our finding on the reduced lipid accumulation and TNF- $\alpha$  release after OLE treatments. The ability of olive oil polyphenols to reduce lipid synthesis in cultured primary hepatocytes has been reported,<sup>75–77</sup> as well as the ability of olive leaf extract to reduce lipid accumulation in cultured hepatic cells.<sup>59</sup> Moreover, olive oil extract has been demonstrated to reduce the amount of LD in the liver of rats fed a high-fat diet.<sup>78</sup> A hypolipidemic effect of olive leaf extract has been also recently reported in a meta-analysis of randomized controlled trials.<sup>79</sup>

Regarding the specific effect of olive oil and its extract on enzymes involved in lipid metabolism, in keeping with our findings, a downregulation of TAG synthesis throughout DGAT inhibition has been demonstrated in rat hepatocytes treated with isolated phenols<sup>76</sup> or with an extract of olive oil.<sup>80</sup> Downregulation of SCD1 gene expression in hyperinsulinemic rats treated with an olive oil-enriched diet has been also demonstrated.<sup>81</sup>

In the last few years, the autophagic process has been strictly correlated with the development and progression of hepatic steatosis. Autophagy has been reported to regulate both LD formation and degradation<sup>82,83</sup> and the degradation of LD by autophagy has been named “lipophagy”.<sup>84</sup> The contribution of autophagic activity toward lipid metabolism and, consequently, to steatosis development is still a matter of intense debate in the literature.

LC3 is a soluble protein ubiquitously present in both mammalian tissues and cultured cells. During autophagy, a cytosolic form of LC3 (LC3-I) is conjugated to phosphatidylethanolamine to form LC3–phosphatidylethanolamine conjugate (LC3-II), which is recruited into autophagosomal membranes.

Autophagosomes, which contain cytoplasmic components, including cytosolic proteins and organelles, fuse with lysosomes to form autolysosomes. Within autolysosomes, cellular components, including LC3-II, are degraded by lysosomal hydrolases.<sup>85</sup> In line with published data,<sup>86</sup> in which reduced lipophagy dependent on a high-fat diet was reported, in our experiments, we found that high FFA induced autophagosomes, as demonstrated by increased LC3-II/LC3-I ratio, and arrested lipophagy due to a significant reduction in the LAMP-1 docked lysosomal component.

OLE addition to FFA-treated cells rescues the lysosome component and LCII/LCI ratio, indicating activation of the degradative pathway. Thus, we hypothesized that OLE, throughout lipophagy activation and changes in the protein expression of enzymes involved in LD metabolism can relieve the lipotoxic pressure and ameliorates parameters of oxidative stress. Our data are in line with those of recent work describing the ability of polyphenol-rich natural products to treat various liver diseases through the regulation of the autophagic process.<sup>87</sup>

Overall, our data provide important results because the use of low temperatures and water makes the olive leaf extract safe and at the same time guarantees the total preservation of its beneficial properties on the liver.

## Author contributions

Conceptualization, A. M. G.; methodology, S. L., C. M., M. F., S. T., G. D., F. G., and F. C.; software, S. T.; validation, A. M. G.; formal analysis, A. R., G. D., V. M. P. and D. V.; investigation, A. M. G., D. L., and L. D.; data curation, S. T. and A. M. G.; writing – original draft preparation, A. M. G.; writing – review and editing, S. T., D. L., D. V., C. B., S. G., and L. D.; supervision, A. M. G., and L. D.; funding acquisition, A. R. All authors have read and agreed to the published version of the manuscript.

## Conflicts of interest

The authors declare no conflict of interest.

## Acknowledgements

Italian Ministry of Education, University and Research, grants to Adele Romano (PRIN 2020SEMP22\_002).

## References

- 1 A. P. Delli Bovi, F. Marciano, C. Mandato, M. A. Siano, M. Savoia and P. Vajro, Oxidative Stress in Non-alcoholic Fatty Liver Disease. An Updated Mini Review, *Front. Med.*, 2021, **8**, 595371.
- 2 H. Shi, M. V. Kokoeva, K. Inouye, I. Tzameli, H. Yin and J. S. Flier, TLR4 links innate immunity and fatty acid-



- induced insulin resistance, *J. Clin. Invest.*, 2006, **116**(11), 3015–3025.
- 3 M. T. A. Nguyen, S. Favellyukis, A. K. Nguyen, D. Reichart, P. A. Scott, A. Jenn, R. Liu-Bryan, C. K. Glass, J. G. Neels and J. M. Olefsky, A subpopulation of macrophages infiltrates hypertrophic adipose tissue and is activated by free fatty acids via Toll-like receptors 2 and 4 and JNK-dependent pathways, *J. Biol. Chem.*, 2007, **282**(48), 35279–35292.
  - 4 C. Andrés Juan, J. Manuel Pérez de la Lastra, F. J. Plou, E. Pérez-Lebeña and S. Reinbothe, The Chemistry of Reactive Oxygen Species (ROS) Revisited: Outlining Their Role in Biological Macromolecules (DNA, Lipids and Proteins) and Induced Pathologies, *Int. J. Mol. Sci.*, 2021, **22**(9), 4642.
  - 5 M. Masarone, V. Rosato, M. Dallio, A. G. Gravina, A. Aglitti, C. Loguercio, A. Federico and M. Persico, Role of Oxidative Stress in Pathophysiology of Nonalcoholic Fatty Liver Disease, *Oxid. Med. Cell. Longevity*, 2018, **2018**, 9547613.
  - 6 M. Vivancos and J. J. Moreno, Effect of resveratrol, tyrosol and beta-sitosterol on oxidised low-density lipoprotein-stimulated oxidative stress, arachidonic acid release and prostaglandin E2 synthesis by RAW 264.7 macrophages, *Br. J. Nutr.*, 2008, **99**(6), 1199–1207.
  - 7 S. N. El and S. Karakaya, Olive tree (*Olea europaea*) leaves: potential beneficial effects on human health, *Nutr. Rev.*, 2009, **67**(11), 632–638.
  - 8 A. Boss, K. S. Bishop, G. Marlow, M. P. G. Barnett and L. R. Ferguson, Evidence to Support the Anti-Cancer Effect of Olive Leaf Extract and Future Directions, *Nutrients*, 2016, **8**(8), 513.
  - 9 Z. Erbay and F. Icier, A review of thin layer drying of foods: theory, modeling, and experimental results, *Crit. Rev. Food Sci. Nutr.*, 2010, **50**(5), 441–464.
  - 10 H. Shirzad, V. Niknam, M. Taheri and H. Ebrahimzadeh, Ultrasound-assisted extraction process of phenolic antioxidants from Olive leaves: A nutraceutical study using RSM and LC–ESI–DAD–MS, *J. Food Sci. Technol.*, 2017, **54**(8), 2631–2371.
  - 11 P. Vogel, I. K. Machado, J. Garavaglia, V. T. Zani, D. de Souza and S. M. Dal Bosco, Polyphenols benefits of olive leaf (*Olea europaea* L) to human health, *Nutr. Hosp.*, 2014, **31**(3), 1427–1433.
  - 12 O. Benavente-García, J. Castillo, J. Lorente, A. Ortuño and J. A. del Rio, Antioxidant activity of phenolics extracted from *Olea europaea* L. leaves, *Food Chem.*, 2000, **68**, 457–462.
  - 13 N. Rahmanian, S. M. Jafari and T. A. Wani, Bioactive profile, dehydration, extraction and application of the bioactive components of olive leaves, *Trends Food Sci. Technol.*, 2015, **42**, 150–172.
  - 14 C. E. Storniolo, N. Martínez-Hovelman, M. Martínez-Huélamo, R. M. Lamuela-Raventos and J. J. Moreno, Extra Virgin Olive Oil Minor Compounds Modulate Mitogenic Action of Oleic Acid on Colon Cancer Cell Line, *J. Agric. Food Chem.*, 2019, **67**(41), 11420–11427.
  - 15 S. K. Yoon, in *The Liver: Oxidative Stress and Dietary Antioxidants*, 2018.
  - 16 X. Pintó, M. Fanlo-Maresma, E. Corbella, X. Corbella, M. T. Mitjavila, J. J. Moreno, R. Casas, R. Estruch, D. Corella, M. Bulló, M. Ruiz-Canela, O. Castañer, J. A. Martínez, E. Ros, M. A. Martínez-González, D. Corella, M. Fitó, J. Salas-Salvadó, F. Arós, M. Aldamiz-Echevarría, Á. M. Alonso-Gómez, J. Berjón, L. Forga, J. Gállego, A. García-Layana, A. Larrauri, J. Portu-Zapirain, J. Timiraos, M. Covas, M. A. Martínez-González, A. Pérez-Heras, M. Serra-Mir, X. Pi-Sunyer, C. A. González, F. B. Hu, J. Sabaté, E. De La Cruz, A. Galera, M. Gimenez-Garcia, H. Lafuente, M. A. Rodríguez-Sanchez, F. Trias, I. Sarasa, R. Figueras, M. Liceran, C. Pallarols, V. Esteve, C. Storniolo, M. Serra-Mir, A. Pérez-Heras, A. Sala-Vila, C. Valls-Pedret, C. Viñas, R. Casas, A. Medina-Remón, S. Romero, J. M. Baena, M. García, M. Oller, J. Amat, I. Duaso, Y. García, C. Iglesias, C. Simón, L. Quinzavos, L. Parra, M. Liroz, J. Benavent, J. Clos, I. Pla, M. Amorós, M. T. Bonet, M. T. Martín, M. S. Sánchez, J. Altirriba, E. Manzano, A. Altés, M. Cofán, M. Doménech, T. M. Freitas-Simoes, I. Roth, A. J. Amor, E. Ortega, J. C. Laguna, M. Alegret, R. Gilabert, N. Bargalló, M. A. Martínez-González, P. Buil-Cosiales, E. Toledo, A. García-Arellano, J. C. Cenoz-Osinaga, O. Lecea-Juárez, C. Razquin, A. Sánchez-Tainta, B. Sanjulián, J. Díez-Espino, I. Zazpe, F. J. Basterra-Gortari, S. Eguaras, E. Goñi, Z. Vazquez, M. Bes-Rastrollo, A. Gea, N. Martín-Calvo, N. Berrade, A. Marti, J. Alfredo Martínez, E. H. Martínez-Lapiscina, M. García-López, S. Cervantes, F. Barcena Amigo, C. Oreja Arrayago, M. J. Lasanta Saez, L. Quintana Pedraza, P. Cia Lecumberri, T. Elcarte Lopez, T. Forcen Alonso, I. Álvarez-Alvarez, M. Guasch-Ferré, R. González, C. Molina, F. Márquez, N. Babio, J. García Roselló, A. Diaz-López, F. Martin, R. Tort, A. Isach, N. Becerra, C. Ferreira, J. J. Cabré, J. Fernández-Ballart, N. Ibarrola-Jurado, G. Mestres, N. Rosique-Esteban, C. Alegret, P. Martínez, S. Millán, J. L. Piñol, T. Basora, A. Salas-Huetos, J. M. Hernández, P. Carrasco, C. Ortega-Azorín, E. M. Asensio, R. Osma, R. Barragán, F. Francés, M. Guillén, J. I. González, C. Sáiz, O. Portolés, F. J. Giménez, O. Coltell, R. Fernández-Carrión, P. Guillem-Sáiz, I. González-Monje, L. Quiles, V. Pascual, C. Riera, M. A. Pages, D. Godoy, A. Carratalá-Calvo, S. Sánchez-Navarro, C. Valero-Barceló, M. Fitó, J. Vila, I. Subirana, S. Tello, R. De La Torre, D. Muñoz-Aguayo, R. Elosua, J. Marrugat, H. Schröder, N. Molina, E. Maestre, A. Rovira, M. Farré, F. Arós, J. Timiraos, I. Salaverría, J. Rekondo, M. C. Belló, T. Del Hierro, J. Algorta, S. Francisco, A. Alonso, J. San Vicente, E. Sanz, I. Felipe, A. Loma-Osorio, E. Gómez-Gracia, J. Fernández-Crehuet, M. Gutiérrez-Bedmar, R. Benítez Pont, M. Bianchi Alba, J. Wärnberg, R. Gómez-Huelgas, J. Martínez-González, V. Velasco García, J. De Diego Salas, A. Baca Osorio, J. Gil Zarzosa, J. J. Sánchez Luque, E. Vargas López, D. Romaguera, M. García-Valdúeza, M. Moñino, A. Yáñez, A. Proenza, R. Prieto, S. Munuera, M. Vivó, F. Bestard, J. A. Munar, L. Coll, F. Fiol, M. Ginard, A. Jover, J. García, M. Leal,



- E. Martínez, J. M. Santos-Lozano, M. Ortega-Calvo, P. Román, F. José García, P. Iglesias, Y. Corchado, L. Mellado, L. Miró-Moriano, J. M. Lozano-Rodríguez, C. Domínguez-Espinaco, S. Vaquero-Díaz, M. C. López-Sabater, A. I. Castellote-Bargalló, P. Quifer-Rada, L. Palmas, J. Álvarez-Pérez, E. M. Díaz-Benítez, A. Sánchez-Villegas, L. T. Casañas-Quintana, J. Pérez-Cabrera, C. Ruano-Rodríguez, I. Bautista-Castaño, F. Sarmiento De La Fe, J. A. García Pastor, B. V. Díaz-González, J. M. Castillo Anzalas, R. E. Sosa-Also, J. Medina-Ponce, C. Cabezas, E. Vinyoles, M. A. Rovira, L. García, G. Flores, J. M. Verdú, P. Baby, A. Ramos, L. Mengual, P. Roura, M. C. Yuste, A. Guarner, A. Rovira, M. I. Santamaría, M. Mata, C. De Juan, A. Brau, V. Ruiz-Gutiérrez, J. Sánchez Perona, E. Montero Romero, M. García-García, E. Jurado-Ruiz, M. P. Portillo, G. Sáez and J. Tur, A Mediterranean Diet Rich in Extra-Virgin Olive Oil Is Associated with a Reduced Prevalence of Nonalcoholic Fatty Liver Disease in Older Individuals at High Cardiovascular Risk, *J. Nutr.*, 2019, **149**(11), 1920–1929.
- 17 A. I. Andres, M. J. Petron, A. M. Lopez and M. L. Timon, Optimization of Extraction Conditions to Improve Phenolic Content and In Vitro Antioxidant Activity in Craft Brewers' Spent Grain Using Response Surface Methodology (RSM), *Foods*, 2020, **9**(10), 1398.
- 18 F. Chemat, M. A. Vian, H. K. Ravi, B. Khadhraoui, S. Hilali, S. Perino and A. S. F. Tixier, Review of Alternative Solvents for Green Extraction of Food and Natural Products: Panorama, Principles, Applications and Prospects, *Molecules*, 2019, **24**(16), 3007.
- 19 N. Ilayaraja, K. R. Likhith, G. R. Sharath Babu and F. Khanum, Optimisation of extraction of bioactive compounds from *Feronia limonia* (wood apple) fruit using response surface methodology (RSM), *Food Chem.*, 2015, **173**, 348–354.
- 20 P. Conte, S. Pulina, A. del Caro, C. Fadda, P. P. Urgeghe, A. de Bruno, G. Difonzo, F. Caponio, R. Romeo and A. Piga, Gluten-Free Breadsticks Fortified with Phenolic-Rich Extracts from Olive Leaves and Olive Mill Wastewater, *Foods*, 2021, **10**(5), 923.
- 21 G. Difonzo, A. Russo, A. Trani, V. M. Paradiso, M. Ranieri, A. Pasqualone, C. Summo, G. Tamma, R. Silletti and F. Caponio, Green extracts from Coratina olive cultivar leaves: Antioxidant characterization and biological activity, *J. Funct. Foods*, 2017, **31**, 63–70.
- 22 M. Centrone, M. D'agostino, G. Difonzo, A. De Bruno, A. Di Mise, M. Ranieri, C. Montemurro, G. Valenti, M. Poiana, F. Caponio and G. Tamma, Antioxidant Efficacy of Olive By-Product Extracts in Human Colon HCT8 Cells, *Foods*, 2021, **10**(1), 11.
- 23 A. A. Spector, Fatty acid binding to plasma albumin, *J. Lipid Res.*, 1975, **16**(3), 165–179.
- 24 A. M. Giudetti, D. Vergara, S. Longo, M. Friuli, B. Eramo, S. Tacconi, M. Fidaleo, L. Dini, A. Romano and S. Gaetani, Oleylethanolamide Reduces Hepatic Oxidative Stress and Endoplasmic Reticulum Stress in High-Fat Diet-Fed Rats, *Antioxidants*, 2021, **10**(8), 1289.
- 25 G. Difonzo, M. A. Crescenzi, S. Piacente, G. Altamura, F. Caponio and P. Montoro, Metabolomics Approach to Characterize Green Olive Leaf Extracts Classified Based on Variety and Season, *Plants*, 2022, **11**(23), 3321.
- 26 A. M. Giudetti, F. Guerra, S. Longo, R. Beli, R. Romano, F. Manganelli, M. Nolano, V. Mangini, L. Santoro and C. Bucci, An altered lipid metabolism characterizes Charcot-Marie-Tooth type 2B peripheral neuropathy, *Biochim. Biophys. Acta, Mol. Cell Biol. Lipids*, 2020, **1865**(12), 158805.
- 27 R. Romano, V. S. del Fiore, P. Saveri, I. E. Palamà, C. Pisciotta, D. Pareyson, C. Bucci and F. Guerra, Autophagy and Lysosomal Functionality in CMT2B Fibroblasts Carrying the RAB7<sup>K126R</sup> Mutation, *Cells*, 2022, **11**(3), 496.
- 28 M. de Luca, R. Romano and C. Bucci, Role of the V1G1 subunit of V-ATPase in breast cancer cell migration, *Sci. Rep.*, 2021, **11**, 4615.
- 29 F. Guerra, A. Paiano, D. Migoni, G. Girolimetti, A. M. Perrone, P. de Iaco, F. P. Fanizzi, G. Gasparre and C. Bucci, Modulation of RAB7A Protein Expression Determines Resistance to Cisplatin through Late Endocytic Pathway Impairment and Extracellular Vesicular Secretion, *Cancers*, 2019, **11**(1), 52.
- 30 R. Marwaha and M. Sharma, DQ-Red BSA trafficking assay in cultured cells to assess cargo delivery to lysosomes, *Bio-Protoc.*, 2017, **7**(19), e2571–e2571.
- 31 M. Salbini, A. Quarta, F. Russo, A. M. Giudetti, C. Citti, G. Cannazza, G. Gigli, D. Vergara and A. Gaballo, Oxidative Stress and Multi-Organ Damage Induced by Two Novel Phytocannabinoids, CBDB and CBDP, in Breast Cancer Cells, *Molecules*, 2021, **26**(18), 5576.
- 32 S. H. Omar, Oleuropein in olive and its pharmacological effects, *Sci. Pharm.*, 2010, **78**, 133–154.
- 33 C. Manna, V. Migliardi, P. Golino, A. Scognamiglio, P. Galletti, M. Chiariello and V. Zappia, Oleuropein prevents oxidative myocardial injury induced by ischemia and reperfusion, *J. Nutr. Biochem.*, 2004, **15**(8), 461–466.
- 34 C. Zhang, E. L. Klett and R. A. Coleman, Lipid signals and insulin resistance, *Clin. Lipidol.*, 2013, **8**(6), 659–667.
- 35 M. Gaggini, M. Morelli, E. Buzzigoli, R. A. DeFronzo, E. Bugianesi and A. Gastaldelli, Non-alcoholic fatty liver disease (NAFLD) and its connection with insulin resistance, dyslipidemia, atherosclerosis and coronary heart disease, *Nutrients*, 2013, **5**(5), 1544–1560.
- 36 J. Zhang, X. Wang, V. Vikash, Q. Ye, D. Wu, Y. Liu and W. Dong, ROS and ROS-Mediated Cellular Signaling, *Oxid. Med. Cell. Longevity*, 2016, **2016**, 4350965.
- 37 G. C. Farrell, D. van Rooyen, L. Gan and S. Chitturi, NASH is an Inflammatory Disorder: Pathogenic, Prognostic and Therapeutic Implications, *Gut Liver*, 2012, **6**(2), 149–171.
- 38 K. Popko, E. Gorska, A. Stelmaszczyk-Emmel, R. Plywaczewski, A. Stoklosa, D. Gorecka, B. Pyrzak and U. Demkow, Proinflammatory cytokines Il-6 and TNF- $\alpha$  and the development of inflammation in obese subjects, *Eur. J. Med. Res.*, 2010, **15**(2), 120–122.



- 39 R. S. Rector, J. P. Thyfault, G. M. Uptergrove, E. M. Morris, S. P. Naples, S. J. Borengasser, C. R. Mikus, M. J. Laye, M. H. Laughlin, F. W. Booth and J. A. Ibdah, Mitochondrial dysfunction precedes insulin resistance and hepatic steatosis and contributes to the natural history of non-alcoholic fatty liver disease in an obese rodent model, *J. Hepatol.*, 2010, **52**(5), 727–736.
- 40 M. Carmiel-Haggai, A. I. Cederbaum and N. Nieto, A high-fat diet leads to the progression of non-alcoholic fatty liver disease in obese rats, *FASEB J.*, 2005, **19**(1), 136–138.
- 41 D. S. Cassarino, J. K. Parks, W. D. Parker and J. P. Bennett, The parkinsonian neurotoxin MPP<sup>+</sup> opens the mitochondrial permeability transition pore and releases cytochrome c in isolated mitochondria via an oxidative mechanism, *Biochim. Biophys. Acta*, 1999, **1453**(1), 49–62.
- 42 F. Guerra and C. Bucci, Multiple Roles of the Small GTPase Rab7, *Cells*, 2016, **5**(3), 34.
- 43 B. Schroeder, R. J. Schulze, S. G. Weller, A. C. Sletten, C. A. Casey and M. A. McNiven, The small GTPase Rab7 as a central regulator of hepatocellular lipophagy, *Hepatology*, 2015, **61**(6), 1896–1907.
- 44 S. W. Kim, W. Hur, T. Z. Li, Y. K. Lee, J. E. Choi, S. W. Hong, K. S. Lyoo, C. R. You, E. S. Jung, C. K. Jung, T. Park, S. J. Um and S. K. Yoon, Oleuropein prevents the progression of steatohepatitis to hepatic fibrosis induced by a high-fat diet in mice, *Exp. Mol. Med.*, 2014, **46**(4), e92.
- 45 T. T. G. Ly, J. Yun, D. H. Lee, J. S. Chung and S. M. Kwon, Protective Effects and Benefits of Olive Oil and Its Extracts on Women's Health, *Nutrients*, 2021, **13**(12), 4279.
- 46 L. Martínez, J. Castillo, G. Ros and G. Nieto, Antioxidant and Antimicrobial Activity of Rosemary, Pomegranate and Olive Extracts in Fish Patties, *Antioxidants*, 2019, **8**(4), 86.
- 47 P. G. Lins, S. Marina Piccoli Pugine, A. M. Scatolini and M. P. de Melo, *In vitro*, antioxidant activity of olive leaf extract (*Olea europaea* L.) and its protective effect on oxidative damage in human erythrocytes, *Heliyon*, 2018, **4**(9), e00805.
- 48 C. E. Storniolo, I. Sacanella, R. M. Lamuela-Raventos and J. J. Moreno, Bioactive Compounds of Mediterranean Cooked Tomato Sauce (Sofrito) Modulate Intestinal Epithelial Cancer Cell Growth Through Oxidative Stress/Arachidonic Acid Cascade Regulation, *ACS Omega*, 2020, **5**(28), 17071–17077.
- 49 M. Robles-Almazan, M. Pulido-Moran, J. Moreno-Fernandez, C. Ramirez-Tortosa, C. Rodriguez-Garcia, J. L. Quiles and M. Ramirez-Tortosa, Bioavailability, toxicity, and clinical applications, *Food Res. Int.*, 2018, **105**, 654–667.
- 50 M. Vivancos and J. J. Moreno, beta-Sitosterol modulates antioxidant enzyme response in RAW 264.7 macrophages, *Free Radicals Biol. Med.*, 2005, **39**, 91–97.
- 51 K. Madan, P. Bhardwaj, S. Thareja, S. D. Gupta and A. Saraya, Oxidant stress and antioxidant status among patients with nonalcoholic fatty liver disease (NAFLD), *J. Clin. Gastroenterol.*, 2006, **40**(10), 930–935.
- 52 G. Tang, Y. Xu, C. Zhang, N. Wang, H. Li and Y. Feng, Green tea and epigallocatechin gallate (EGCG) for the management of nonalcoholic fatty liver diseases (NAFLD): Insights into the role of oxidative stress and antioxidant mechanism, *Antioxidants*, 2021, **10**(7), 1076.
- 53 V. Musolino, R. Macri, A. Cardamone, M. Serra, A. R. Coppoletta, L. Tucci, J. Maiuolo, C. Lupia, F. Scarano, C. Carresi, S. Nucera, I. Bava, M. Marrelli, E. Palma, M. Gliozzi and V. Mollace, Nocellara Del Belice (*Olea europaea* L. Cultivar): Leaf Extract Concentrated in Phenolic Compounds and Its Anti-Inflammatory and Radical Scavenging Activity, *Plants*, 2023, **12**(1), 27.
- 54 K. Omagari, S. Kato, K. Tsuneyama, H. Hatta, M. Sato, M. Hamasaki, Y. Sadakane, T. Tashiro, M. Fukuhata, Y. Miyata, S. Tamaru, K. Tanaka and M. Mune, Olive leaf extract prevents spontaneous occurrence of non-alcoholic steatohepatitis in SHR/NDmcr-cp rats, *Pathology*, 2010, **42**(1), 66–72.
- 55 H. Saiah, W. Saiah, M. Mokhtar and T. Aburjai, Antioxidant and hepatoprotective potentials of olive (*Olea europaea* L. var. Sigoise) leaves against carbon tetrachloride-induced hepatic damage in rats, and investigation of its constituents by high-performance liquid chromatography-mass spectrometry, *Int. Food Res. J.*, 2022, **29**(3), 607–618.
- 56 C. E. Storniolo, J. Roselló-Catafau, X. Pintó, M. T. Mitjavila and J. J. Moreno, Polyphenol fraction of extra virgin olive oil protects against endothelial dysfunction induced by high glucose and free fatty acids through modulation of nitric oxide and endothelin-1, *Redox Biol.*, 2014, **2**, 971–977.
- 57 D. B. Zorov, C. R. Filburn, L. O. Klotz, J. L. Zweier and S. J. Sollott, Reactive oxygen species (ROS)-induced ROS release: a new phenomenon accompanying induction of the mitochondrial permeability transition in cardiac myocytes, *J. Exp. Med.*, 2000, **192**(7), 1001–1014.
- 58 G. Serviddio, A. M. Giudetti, F. Bellanti, P. Priore, T. Rollo, R. Tamborra, L. Siculella, G. Vendemiale, E. Altomare and G. V. Gnoni, Oxidation of hepatic carnitine palmitoyl transferase-I (CPT-I) impairs fatty acid beta-oxidation in rats fed a methionine-choline deficient diet, *PLoS One*, 2011, **6**(9), e24084.
- 59 I. Burò, V. Consoli, A. Castellano, L. Vanella and V. Sorrenti, Beneficial Effects of Standardized Extracts from Wastes of Red Oranges and Olive Leaves, *Antioxidants*, 2022, **11**(8), 1496.
- 60 N. Yazihan, S. Akdas, Y. Olgar, D. Biriken, B. Turan and M. T. Ozkaya, Olive oil attenuates oxidative damage by improving mitochondrial functions in human keratinocytes, *J. Funct. Foods*, 2020, **71**, 104008.
- 61 E. Chiaino, M. Micucci, R. Budriesi, L. B. Mattioli, C. Marzetti, M. Corsini and M. Frosini, Hibiscus Flower and Olive Leaf Extracts Activate Apoptosis in SH-SY5Y Cells, *Antioxidants*, 2021, **10**(12), 1962.
- 62 N. Lemonakis, V. Mougios, M. Halabalaki, I. Dagla, A. Tsarbopoulos, A. L. Skaltsounis and E. Gikas, Effect of Supplementation with Olive Leaf Extract Enriched with



- Oleuropein on the Metabolome and Redox Status of Athletes' Blood and Urine-A Metabolomic Approach, *Metabolites*, 2022, **12**(2), 195.
- 63 M. J. Morgan and Z. G. Liu, Crosstalk of reactive oxygen species and NF- $\kappa$ B signaling, *Cell Res.*, 2011, **21**(1), 103–115.
- 64 A. Oeckinghaus and S. Ghosh, The NF-kappaB family of transcription factors and its regulation, *Cold Spring Harbor Perspect. Biol.*, 2009, **1**(4), a000034.
- 65 T. Liu, L. Zhang, D. Joo and S. C. Sun, NF- $\kappa$ B signaling in inflammation, *Signal Transduction Targeted Ther.*, 2017, **2**, 17023.
- 66 B. Burja, T. Kuret, T. Janko, D. Topalović, L. Živković, K. Mrak-Poljšak, B. Spremo-Potparević, P. Žigon, O. Distler, S. Čučnik, S. Sodin-Semrl, K. Lakota and M. Frank-Bertoncelj, Olive Leaf Extract Attenuates Inflammatory Activation and DNA Damage in Human Arterial Endothelial Cells, *Front. Cardiovasc. Med.*, 2019, **6**, 56.
- 67 L. Giovannelli, Beneficial Effects of Olive Oil Phenols on the Aging Process: Experimental Evidence and Possible Mechanisms of Action, *Nutr. Aging*, 2012, **1**, 207–223.
- 68 S. M. Jeyakumar and A. Vajreswari, Stearoyl-CoA desaturase 1: A potential target for non-alcoholic fatty liver disease?—Perspective on emerging experimental evidence, *World J. Hepatol.*, 2022, **14**, 168–179.
- 69 A. Aljohani, M. I. Khan, A. Bonneville, C. Guo, J. Jeffery, L. O'Neill, D. N. Syed, S. A. Lewis, M. Burhans, H. Mukhtar and J. M. Ntambi, Hepatic stearoyl CoA desaturase 1 deficiency increases glucose uptake in adipose tissue partially through the PGC-1 $\alpha$ -FGF21 axis in mice, *J. Biol. Chem.*, 2019, **294**(51), 19475–19485.
- 70 S. C. Cheol, D. B. Savage, A. Kulkarni, X. Y. Xing, Z. X. Liu, K. Morino, S. Kim, A. Distefano, V. T. Samuel, S. Neschen, D. Zhang, A. Wang, X. M. Zhang, M. Kahn, G. W. Cline, S. K. Pandey, J. G. Geisler, S. Bhanot, B. P. Monia and G. I. Shulman, Suppression of diacylglycerol acyltransferase-2 (DGAT2), but not DGAT1, with antisense oligonucleotides reverses diet-induced hepatic steatosis and insulin resistance, *J. Biol. Chem.*, 2007, **282**, 22678–22688.
- 71 M. Tardelli, Monoacylglycerol lipase reprograms lipid precursors signaling in liver disease, *World J. Gastroenterol.*, 2020, **26**, 3577–3585.
- 72 J. W. Wu, S. P. Wang, F. Alvarez, S. Casavant, N. Gauthier, L. Abed, K. G. Soni, G. Yang and G. A. Mitchell, Deficiency of liver adipose triglyceride lipase in mice causes progressive hepatic steatosis, *Hepatology*, 2011, **54**(1), 122–132.
- 73 S. M. Turpin, A. J. Hoy, R. D. Brown, C. Garcia Rudaz, J. Honeyman, M. Matzaris and M. J. Watt, Adipose triacylglycerol lipase is a major regulator of hepatic lipid metabolism but not insulin sensitivity in mice, *Diabetologia*, 2011, **54**(1), 146–156.
- 74 D. K. Nomura, B. E. Morrison, J. L. Blankman, J. Z. Long, S. G. Kinsey, M. C. G. Marcondes, A. M. Ward, Y. K. Hahn, A. H. Lichtman, B. Conti and B. F. Cravatt, Endocannabinoid hydrolysis generates brain prostaglandins that promote neuroinflammation, *Science*, 2011, **334**(6057), 809–813.
- 75 P. Priore, A. Cavallo, A. Gnoni, F. Damiano, G. V. Gnoni and L. Siculella, Modulation of hepatic lipid metabolism by olive oil and its phenols in nonalcoholic fatty liver disease, *IUBMB Life*, 2015, **67**(1), 9–17.
- 76 P. Priore, L. Siculella and G. V. Gnoni, Extra virgin olive oil phenols down-regulate lipid synthesis in primary-cultured rat-hepatocytes, *J. Nutr. Biochem.*, 2014, **25**, 683–691.
- 77 A. Gnoni, S. Longo, F. Damiano, G. V. Gnoni and A. M. Giudetti, in *Olives and Olive Oil in Health and Disease Prevention*, ed. V. R. Preedy and R. Watson, 2nd edn, 2020.
- 78 H. Poudyal, F. Campbell and L. Brown, Olive leaf extract attenuates cardiac, hepatic, and metabolic changes in high carbohydrate-, high fat-fed rats, *J. Nutr.*, 2010, **140**(5), 946–953.
- 79 E. Razmpoosh, S. Abdollahi, M. Mousavirad, C. C. T. Clark and S. Soltani, The effects of olive leaf extract on cardiovascular risk factors in the general adult population: a systematic review and meta-analysis of randomized controlled trials, *Diabetol. Metab. Syndr.*, 2022, **14**, 151.
- 80 P. Priore, D. Caruso, L. Siculella and G. V. Gnoni, Rapid down-regulation of hepatic lipid metabolism by phenolic fraction from extra virgin olive oil, *Eur. J. Nutr.*, 2015, **54**(5), 823–833.
- 81 X. Deng, M. B. Elam, H. G. Wilcox, L. M. Cagen, E. A. Park, R. Raghov, D. Patel, P. Kumar, A. Sheybani and J. C. Russell, Dietary olive oil and menhaden oil mitigate induction of lipogenesis in hyperinsulinemic corpulent JCR:LA-cp rats: microarray analysis of lipid-related gene expression, *Endocrinology*, 2004, **145**, 5847–5861.
- 82 W. J. Kwanten, W. Martinet, P. P. Michielsen and S. M. Francque, Role of autophagy in the pathophysiology of nonalcoholic fatty liver disease: A controversial issue, *World J. Gastroenterol.*, 2014, **20**, 7325–7338.
- 83 R. Singh and A. M. Cuervo, Autophagy in the cellular energetic balance, *Cell Metab.*, 2011, **13**(5), 495–504.
- 84 R. Singh, S. Kaushik, Y. Wang, Y. Xiang, I. Novak, M. Komatsu, K. Tanaka, A. M. Cuervo and M. J. Czaja, Autophagy regulates lipid metabolism, *Nature*, 2009, **458**(7242), 1131–1135.
- 85 I. Tanida, T. Ueno and E. Kominami, LC3 and Autophagy, *Methods Mol. Biol.*, 2008, **445**, 77–88.
- 86 J. A. Rodriguez-Navarro, S. Kaushik, H. Koga, C. Dall'Armi, G. Shui, M. R. Wenk, G. di Paolo and A. M. Cuervo, Inhibitory effect of dietary lipids on chaperone-mediated autophagy, *Proc. Natl. Acad. Sci. U. S. A.*, 2012, **109**, e705–e714.
- 87 G. Fan, F. Li, P. Wang, X. Jin and R. Liu, Natural-Product-Mediated Autophagy in the Treatment of Various Liver Diseases, *Int. J. Mol. Sci.*, 2022, **23**(23), 15109.

